

Water Droplet Microlightning Enables Catalyst-Free Alkane Dehydrogenation under Ambient Conditions

Yuanyi He, Jinheng Xu, Lecheng Lyu, Yu Xia,* Richard N. Zare,* and Yifan Meng*

Cite This: <https://doi.org/10.1021/acssuschemeng.6c01846>

Read Online

ACCESS |



Metrics & More



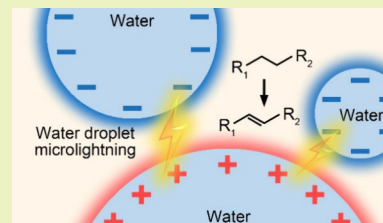
Article Recommendations



Supporting Information

ABSTRACT: We report that microlightning generated between oppositely charged microdroplets during the spraying of pure water surrounded by alkane vapor can initiate catalyst-free alkane dehydrogenation under ambient conditions. When cyclohexane (C_6H_{12}) vapor is introduced into the water spray, a series of dehydrogenated products including cyclohexenyl ($C_6H_9^+$), cyclohexadienyl ($C_6H_7^+$), and phenyl ($C_6H_5^+$) cations are detected by high-resolution mass spectrometry. Control experiments establish that both water and molecular oxygen are essential for this transformation to occur. The capture of alkyl radical intermediates by mass spectrometry suggests that the dehydrogenation proceeds through microlightning-induced radical pathways. Furthermore, the reaction can be scaled up, achieving alkene formation rates of up to 12 mM h^{-1} as quantified by gas chromatography. Beyond cyclohexane, similar dehydrogenation is also observed for other aliphatic substrates. These findings demonstrate a catalyst-free and sustainable method for alkane dehydrogenation under ambient conditions.

KEYWORDS: dehydrogenation, microlightning, gas–water interface, water droplets, cyclohexane



Alkane dehydrogenation represents a fundamental transformation in chemical synthesis, providing direct access to alkenes that serve as key intermediates to produce fuels, polymers, and value-added chemicals.^{1–3} For example, representative market prices for olefin products are typically several-fold higher than those of the corresponding light alkane feedstocks.⁴ However, the activation of strong, nonpolar $C(sp^3)\text{-H}$ bonds in alkanes remains challenging owing to their high bond dissociation energies and low reactivity. Catalyst-based alkane dehydrogenation has been well established as an efficient strategy for converting alkanes into alkenes.^{5–9} Beyond catalytic approaches, plasma-assisted dehydrogenation has emerged as an alternative strategy, where energetic electrons and reactive species generated in plasma environments enable $C\text{-H}$ bond activation under comparatively mild conditions.^{10–12} These studies highlight the potential of nonthermal, plasma-like processes for alkane dehydrogenation.

In parallel, increasing attention has been focused on the unique physical and chemical behavior of gas–liquid and other heterogeneous water interfaces, which can differ strikingly from that of bulk water.^{13–22} One possible explanation is that contact electrification and strong interfacial electric fields at the interface promote the generation of highly reactive transient species, including radicals, electrons, and reactive oxygen species.^{23–27} Recent studies have further shown that the atomization of water into microdroplets can lead to charge separation and electrical discharges between oppositely charged droplets, and thus to a localized, plasma-like environment, which can excite, dissociate, and ionize surrounding gases.^{28–32} This phenomenon, referred to as

water droplet microlightning, represents an interesting mechanism of interfacial electrification-driven reactivity. Distinct from traditional electrospray or plasma, water droplet microlightning is an electrical discharge driven by contact electrification during atomization without the need for external voltage or electrodes. Related discharge phenomena have also been reported at liquid–solid–gas triple-phase interfaces, highlighting the generality of such electrification effects across heterogeneous systems.³³

In this study, we explore whether microlightning generated during the spraying of pure water microdroplets can be utilized to achieve activation of $C\text{-H}$ bond in relatively inert alkanes. Unlike conventional plasma systems, water droplet microlightning arises without external electrodes or applied voltages and exists only locally within the microdroplet spray. We reasoned that such a plasma-like environment, rich in energetic electrons and short-lived radicals, could enable alkane dehydrogenation under ambient conditions. By introducing alkane vapors into the microlightning region, we demonstrate catalyst-free alkane dehydrogenation leading to the formation of unsaturated hydrocarbons. This approach provides a catalyst-free and green method for alkane dehydrogenation under ambient conditions.

Received: February 11, 2026

Revised: March 30, 2026

Accepted: March 31, 2026

Figure 1 illustrates the experimental setup for alkane dehydrogenation induced by water droplet microlightning.

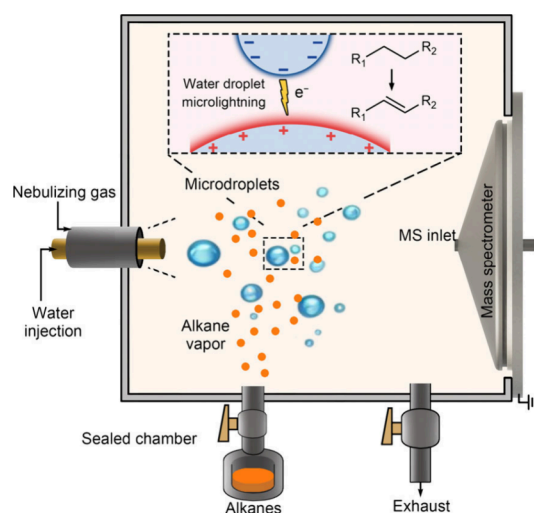


Figure 1. Experimental setup of alkane dehydrogenation by water droplet microlightning.

Pure water was pneumatically sprayed into a sealed chamber to generate microdroplets which were chemically analyzed by mounting the spray source in front of a mass spectrometer. During the spraying process, charge separation among the microdroplets leads to microlightning events within the chamber. The occurrence of discharge events in this system has been previously characterized by a high-speed camera.²⁸ Alkane vapors were introduced into the chamber by free evaporation of the liquid substrates, allowing the gaseous

alkanes to interact with the microlightning region generated by the water spray. The reaction products formed in the gas phase were directly analyzed by mass spectrometry (MS) without any post-treatment. Experimental details are shown in Supplementary Note 1.

Using this setup, we first investigated microlightning-induced dehydrogenation of cyclohexane. Figure 2A schematically illustrates the dehydrogenation of cyclohexane (C_6H_{12}) driven by water droplet microlightning to form the unsaturated hydrocarbon products, cyclohexene (C_6H_{10}), 1,3-cyclohexadiene (C_6H_8), and benzene (C_6H_6). Prior to mass spectrometric analysis, the chamber was evacuated to remove residual air. Upon introduction of the nebulizing gas, the gas atmosphere inside the chamber was defined by the selected nebulizing gas. When cyclohexane vapor was introduced into the reaction chamber and water was nebulized by O_2 , the radical cations of cyclohexane ($C_6H_{12}^+$ at m/z 84.0934) and cyclohexyl ($C_6H_{11}^+$ at m/z 83.0856) were detected by high-resolution MS (Figure 2B). These peaks arise from the reactant (cyclohexane) shown in Figure 2A. In addition, cyclohexenyl cation ($C_6H_9^+$ at m/z 81.0700), cyclohexadienyl cation ($C_6H_7^+$ at m/z 79.0532), and phenyl cation ($C_6H_5^+$ at m/z 77.0376) were also observed when spraying water microdroplets by O_2 into cyclohexane vapor, which indicates the dehydrogenation of cyclohexane. In contrast, when N_2 was used as the nebulizing gas, signals corresponding to dehydrogenated products were not detected, and the spectrum was dominated by cyclohexyl-related ions (Figure 2C). These results suggest that molecular oxygen is essential for microlightning-driven dehydrogenation. Quantitative analysis of the relative intensity ratio of $C_6H_9^+$ to $C_6H_{11}^+$ under different nebulizing gases further confirms the critical role of oxygen. As shown in Figure 2D, dehydrogenation was almost not observed

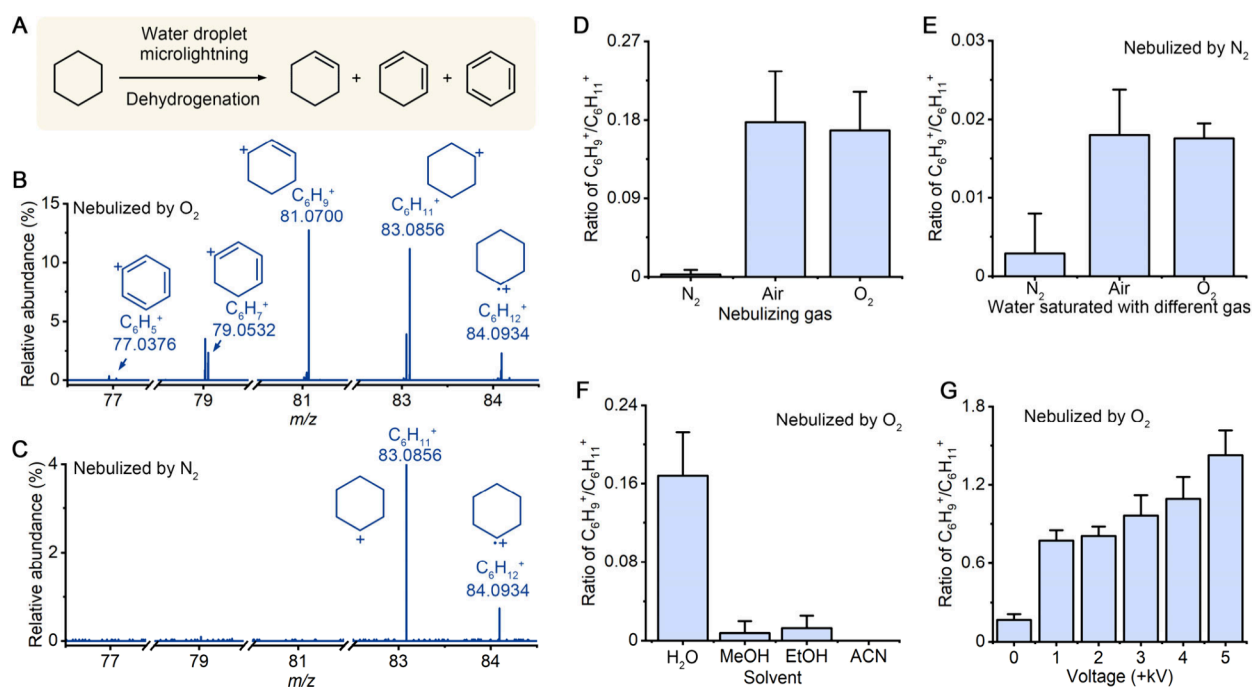


Figure 2. In situ mass spectrometric detection of cyclohexane dehydrogenation induced by water droplet microlightning. (A) Reaction scheme. Mass spectrum when spraying water microdroplets to cyclohexane vapor nebulized by (B) O_2 and (C) N_2 , respectively. Intensity ratio of $C_6H_9^+$ at m/z 81.0700 to $C_6H_{11}^+$ at m/z 83.0856 when using (D) different nebulizing gases, (E) different gas-saturated water, (F) different air-saturated solvents, and (G) different voltage applied to the sprayer. Error bars represent one standard deviation calculated from three independent measurements, $n = 3$.

under N_2 conditions, while both air and O_2 support efficient product formation. However, when water was presaturated with O_2 or air, dehydrogenation was also observed even when N_2 was employed as the nebulizing gas (Figure 2E). Notably, neither the cations of the reactant nor the dehydrogenation products were observed when spraying water droplets containing dissolved cyclohexane (Figure S1), supporting that the dominant ionization and dehydrogenation events occur in the gas-phase region between microdroplets—that is, the region where microlightning occurs.

Figure 2F shows the production formation when spraying different air-saturated solvents to cyclohexane vapor. Compared to acetonitrile (ACN), ethanol (EtOH), and methanol (MeOH) droplets, spraying water microdroplets results in significantly stronger dehydrogenation signals. This difference is likely related to the unique charge separation and microlightning behavior of water droplets during atomization, which appears to be absent or significantly weaker for the organic solvents examined. The influence of an externally applied sprayer voltage on product formation was investigated, showing that higher voltages promote alkane dehydrogenation (Figure 2G). However, to reduce energy consumption and isolate the contribution from water droplet microlightning, all other experiments were conducted without applying external voltage.

It is well established that alkane dehydrogenation under plasma conditions involves radical pathways.¹² Because microlightning generated from water microdroplets exhibits strong similarities to conventional plasma environments, we carried out the following studies to explore the mechanism of microlightning-induced dehydrogenation. 2,2,6,6-tetramethylpiperidine 1-oxyl (TEMPO), which is a radical scavenger, was dissolved in water (100 μM) and sprayed to cyclohexane vapor. As shown in Figure 3, several ion signals corresponding

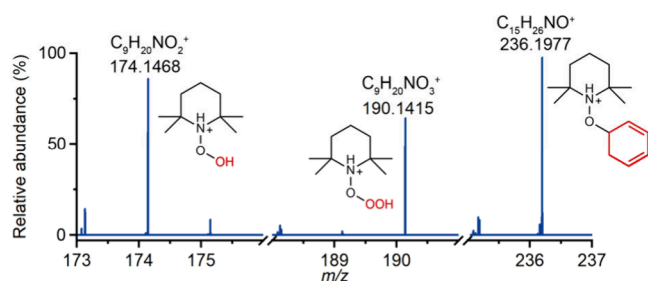


Figure 3. Mass spectrum when spraying TEMPO-contained water into cyclohexane vapor.

to TEMPO-derived adducts were detected by high-resolution MS. The signal at m/z 174.1468 is assigned to $[\text{TEMPO}+\text{OH}]^+$, while the peak at m/z 190.1415 corresponds to $[\text{TEMPO}+\text{OOH}]^+$ adduct. Moreover, the peak at m/z 236.1977 is attributed to the adduct of TEMPO and cyclohexadienyl radical. The detection of these short-lived radical intermediates by MS supports the involvement of radical pathways in microlightning-induced alkane dehydrogenation.

In this system, water microdroplets function as a physical medium and energy transducer to facilitate C–H bond activation rather than acting as a traditional chemical catalyst. Furthermore, positive nanoelectrospray ionization (nESI) experiments demonstrate that positively charged droplets can also initiate alkane dehydrogenation (Figure S2), which is

likely driven by the high interfacial electric field at the droplet surface.³⁴ The generation of such fields is consistent with iontronic principles involving collective ionic asymmetry during droplet deformation.³⁵

To evaluate whether microlightning-induced alkane dehydrogenation can proceed beyond transient events and lead to sustained product accumulation, we performed scale-up experiments under continuous spraying conditions. One mL cyclohexane and 10 mL water were added into a sealed glass vial, followed by gas exchange to establish the desired atmosphere. An atomizer was used to generate water microdroplets containing cyclohexane (Figure S3). In Figure 4A, the black line represents the ultraviolet–visible (UV–Vis) spectrum of the homogeneous emulsion without nebulizing. The red line and blue line represent the UV–vis spectrum of organic layer that was collected from the homogeneous emulsion after 2-h nebulization and a standard mixture of cyclohexene, cyclohexadiene, and benzene (volume ratio 1:1:1) (Figure S4). The red line shows the emergence of distinct absorption features in the 230–270 nm region. These features are absent prior to spraying and closely resemble those of the standard mixture, indicating the accumulation of unsaturated hydrocarbon products during the reaction.

Gas chromatography (GC) analysis further confirms the formation of these dehydrogenation products. After 5 h of continuous nebulizing, chromatograms obtained under both air and O_2 nebulization exhibit peaks corresponding to cyclohexene, cyclohexadiene, and benzene, with retention times matching those of standards (Figure 4B). The identification of GC peaks is shown in Figure S5. As demonstrated in Figure 4C, quantitative analysis of product concentrations as a function of nebulizing time reveals a near-linear increase over the 5 h reaction period under atmospheric conditions. Cyclohexene accumulates at a rate of 9.35 mM h^{-1} , while cyclohexadiene and benzene form at rates of 0.54 and 0.62 mM h^{-1} , respectively. Calibration curves of the quantification of these three products are shown in Figures S6–S8. Under O_2 nebulization, the formation rates increase to 12.65 mM h^{-1} for cyclohexene, 0.70 mM h^{-1} for cyclohexadiene, and 1.30 mM h^{-1} for benzene (Figure 4D). Compared to air, the higher oxygen concentration enhances both the reaction rate and extent, accelerating the dehydrogenation process and increasing the relative abundance of benzene. The detailed influence of oxygen concentration on the reaction performance warrants further investigation. The linearity of the quantitative results obtained under O_2 nebulization is slightly poorer than that observed under air. This deviation is likely owing to minor fluctuations in the oxygen concentration inside the spray chamber, which may arise from imperfect sealing of the chamber. These results demonstrate that microlightning-induced alkane dehydrogenation can be sustained over extended time scales, leading to continuous accumulation of dehydrogenated products.

In addition, the H_2 in the gas phase was identified and quantified after reaction by GC. The formation rate of H_2 was 1.08 $\mu\text{mol/h}$ (Figure S9), accounting for approximately one-tenth of the total dehydrogenation. This suggests a dual-pathway mechanism: a primary oxidative pathway that generates H_2O , and a nonoxidative pathway that releases H_2 . No overoxidation or cracking products, including CO, C_2H_4 , and C_3H_6 , were detected after reaction.

This system exhibits high conversion efficiency for alkane dehydrogenation. To demonstrate this, 4 μL (37.08 μmol) of

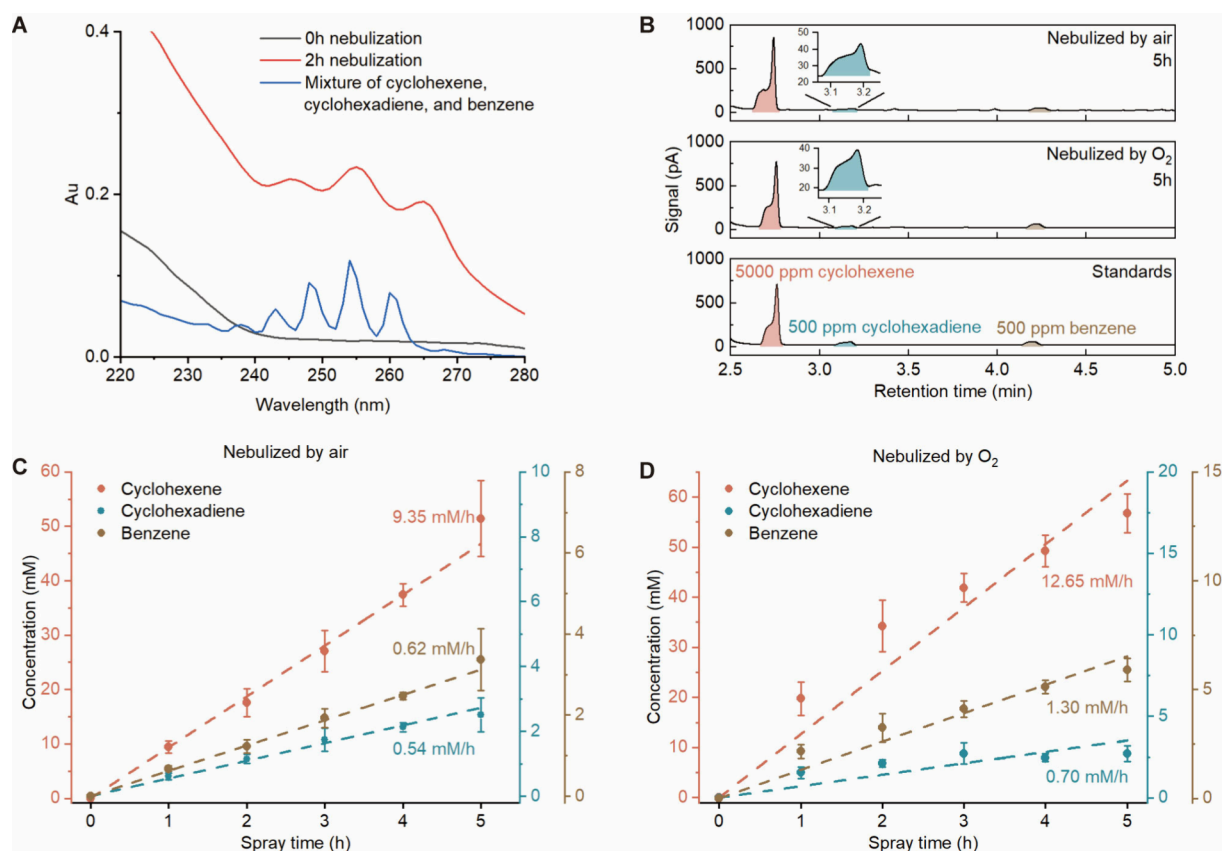


Figure 4. Scale up cyclohexane dehydrogenation induced by water droplet microlightning. (A) UV-vis spectra of cyclohexane-contained water collected before spraying, after 2 h of continuous spraying, and a reference mixture. (B) GC analysis of products formed after 5 h of continuous spraying when nebulized by air and O₂, together with chromatograms of standards for comparison. (C) Time-dependent accumulation of cyclohexene, cyclohexadiene, and benzene during continuous spraying when air is used as the nebulizing gas. (D) Time-dependent accumulation of cyclohexene, cyclohexadiene, and benzene during continuous spraying when O₂ is used as the nebulizing gas. Error bars represent one standard deviation calculated from three independent measurements, $n = 3$.

cyclohexane in 10 mL of H₂O was nebulized for 5 h. The majority of the precursor was converted to a mixture of cyclohexene (18.10 μ mol) and benzene (16.31 μ mol). The total yield of dehydrogenated products reached 93%, confirming the high efficiency of the process for treating a fixed amount of alkane precursor.

These scale-up results underscore the potential of water droplet microlightning as a sustainable platform for industrial alkene production. We estimate the energy cost for this transformation to be approximately 7076 MJ/mol, which is comparable to reported values (500–5000 MJ/mol) for established plasma-assisted dehydrogenation schemes.¹² Notably, while standard plasma systems typically require high-voltage power supplies and noble gases such as argon, our approach achieves similar performance using only water and a low-cost (\sim \\$1) atomizer. It should be emphasized that these preliminary results were obtained without dedicated optimization of the energy cost or product yield. Further refinements of the spray parameters and chamber geometry are expected to significantly enhance the overall efficiency of this catalyst-free process.

To examine the generality of microlightning-induced alkane dehydrogenation, a series of linear, cyclic, and functionalized aliphatic substrates were also investigated (Figure 5). When spraying microdroplets to *n*-hexane vapor in the sealed chamber, mass spectrometric analysis revealed the formation of dehydrogenated products corresponding to mono- and

diunsaturated C₆ species. As shown in Figure 5A, the peaks of C₆H₁₁⁺ at m/z 83.0843 and C₆H₉⁺ at m/z 81.0688 represent hexene and hexadiene, respectively. Tandem mass spectrum of the peak at m/z 83.0843 confirms the position of the formed C = C double bond (Figure S10). Similar dehydrogenation behavior was also observed for *n*-pentane, which yields C₅H₉⁺ at m/z 69.0689 and C₅H₇⁺ at m/z 67.0534 corresponding to unsaturated C₅ products. For cyclopentane, the mass spectrum shows signals attributable to cyclopentenyl cation (C₅H₇⁺ at m/z 67.0532) and cyclopentene radical cation (C₅H₈⁺ at m/z 68.0611) when spraying water microdroplets to cyclopentane vapor (Figure 5C). Notably, no cyclopentadienyl cation (C₅H₅⁺) was detected during cyclopentane dehydrogenation. This absence may be related to the inherent instability of the cyclopentadienyl cation,³⁶ which is expected to be antiaromatic and therefore highly unfavorable. The scope of microlightning-induced dehydrogenation further extends to functionalized aliphatic substrates. When 2-cyclohexyl-ethylamine was used as the substrate, dehydrogenated products were also detected by the observation of C₈H₁₄N⁺ at m/z 124.1103 and C₈H₁₆N⁺ at m/z 126.1261. More examples of alkane dehydrogenation induced by water droplet microlightning are shown in Figures S11–S13. These results demonstrate that microlightning-induced alkane dehydrogenation is a general transformation that can occur across a wide range of alkanes.

In summary, we show that microlightning generated during the spraying of water microdroplets can initiate catalyst-free

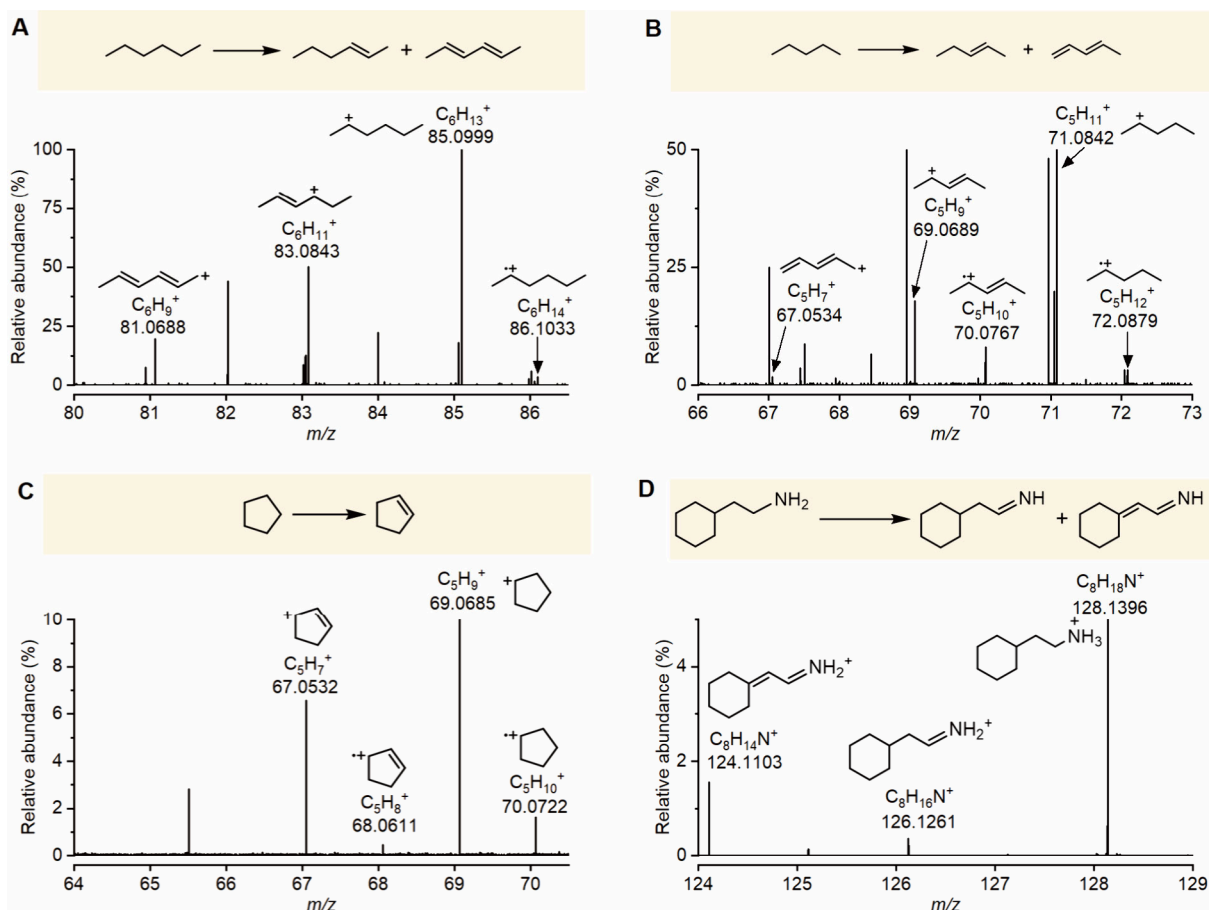


Figure 5. Water droplet microdroplet-induced dehydrogenation of other alkane substrates. (A–D) Mass spectrum when spraying water microdroplets to *n*-hexane, *n*-pentane, cyclopentane, and 2-cyclohexylethylamine, respectively.

alkane dehydrogenation under ambient conditions. A range of linear, cyclic, and functionalized aliphatic substrates undergo stepwise hydrogen removal, leading to the formation of unsaturated hydrocarbons that can be detected by MS. The reaction efficiency is strongly influenced by the presence of O_2 , either in the gas phase or dissolved in water. Like conventional plasma-assisted dehydrogenation, microdroplet-induced alkane dehydrogenation is likely to proceed through radical pathways, as several key radical intermediates were captured by MS. Additionally, the transformation can be scaled up to an alkene formation rate of 12 mM h^{-1} when using cyclohexane as the reagent. Given that representative market prices for olefin products are much higher than those of the corresponding light alkane feedstocks, the development of microdroplet chemistry as a strategy for alkane-to-alkene conversion represents an important industrial opportunity that operates without catalysts, without coke production, and under ambient conditions. This proof-of-concept establishes a foundation for future engineering optimization to achieve the throughput necessary for commercial-scale applications.

ASSOCIATED CONTENT

Supporting Information

The Supporting Information is available free of charge at <https://pubs.acs.org/doi/10.1021/acssuschemeng.6c01846>.

Experimental details; calibration curve for product formation rate; mass spectrometric analysis of more substrates (PDF)

AUTHOR INFORMATION

Corresponding Authors

Yu Xia – School of Environment and Health, Jiangnan University, Wuhan 430056, China; orcid.org/0000-0001-7647-4921; Email: xiayu@jhu.edu.cn

Richard N. Zare – Department of Chemistry, Stanford University, Stanford, California 94305, United States; orcid.org/0000-0001-5266-4253; Email: zare@stanford.edu

Yifan Meng – Frontiers Science Centre for New Organic Matter, Tianjin Key Laboratory of Biosensing and Molecular Recognition, College of Chemistry, Nankai University, Tianjin 300071, China; orcid.org/0000-0001-6897-3595; Email: yfmeng@nankai.edu.cn

Authors

Yuanyi He – Frontiers Science Centre for New Organic Matter, Tianjin Key Laboratory of Biosensing and Molecular Recognition, College of Chemistry, Nankai University, Tianjin 300071, China; Department of Chemistry, Stanford University, Stanford, California 94305, United States; orcid.org/0009-0008-5793-1988

Jinheng Xu – Department of Chemistry, Stanford University, Stanford, California 94305, United States; orcid.org/0009-0007-1187-5389

Lecheng Lyu – Department of Chemistry, Stanford University, Stanford, California 94305, United States; orcid.org/0009-0009-0599-700X

Complete contact information is available at:
<https://pubs.acs.org/10.1021/acssuschemeng.6c01846>

Author Contributions

The manuscript was written through contributions of all authors.

Notes

The authors declare no competing financial interest.

ACKNOWLEDGMENTS

Y.M. acknowledges financial support by College of Chemistry and the Frontiers Science Center for New Organic Matter at Nankai University. Y.X. acknowledges the National Natural Science Foundation of China (22306073 and 22576082). R.N.Z. acknowledges the support by the Air Force Office of Scientific Research through the Multidisciplinary University Research Initiative (MURI) program (AFOSR FA9550-21-1-0170).

REFERENCES

- (1) Bond, J. Q.; Alonso, D. M.; Wang, D.; West, R. M.; Dumesic, J. A. Integrated Catalytic Conversion of γ -Valerolactone to Liquid Alkenes for Transportation Fuels. *Science* **2010**, *327* (5969), 1110–1114.
- (2) Yasuda, H.; Nakamura, A. Diene, Alkyne, Alkene, and Alkyl Complexes of Early Transition Metals: Structures and Synthetic Applications in Organic and Polymer Chemistry. *Angewandte Chemie International Edition in English* **1987**, *26* (8), 723–742.
- (3) Davarnejad, R. *Alkenes: Recent Advances, New Perspectives and Applications*; 2021.
- (4) Ethane to outpace growth in all other U.S. petroleum product consumption through 2023. <https://www.eia.gov/todayinenergy/detail.php?id=51938> (accessed 2026-03-30).
- (5) Sattler, J. J. H. B.; Ruiz-Martinez, J.; Santillan-Jimenez, E.; Weckhuysen, B. M. Catalytic Dehydrogenation of Light Alkanes on Metals and Metal Oxides. *Chem. Rev.* **2014**, *114* (20), 10613–10653.
- (6) Li, C.; Wang, G. Dehydrogenation of light alkanes to monoolefins. *Chem. Soc. Rev.* **2021**, *50* (7), 4359–4381.
- (7) Findlater, M.; Choi, J.; Goldman, A. S.; Brookhart, M. Alkane Dehydrogenation. In *Alkane C-H Activation by Single-Site Metal Catalysis*, Pérez, P. J., Ed.; Springer Netherlands: Dordrecht, 2012; pp 113–141.
- (8) Haenel, M. W.; Oevers, S.; Angermund, K.; Kaska, W. C.; Fan, H.-J.; Hall, M. B. Thermally Stable Homogeneous Catalysts for Alkane Dehydrogenation. *Angew. Chem., Int. Ed.* **2001**, *40* (19), 3596–3600.
- (9) Zhang, L.; Liu, L.; Pan, Z.; Zhang, R.; Gao, Z.; Wang, G.; Huang, K.; Mu, X.; Bai, F.; Wang, Y.; Zhang, W.; Cui, Z.; Li, L. Visible-light-driven non-oxidative dehydrogenation of alkanes at ambient conditions. *Nature Energy* **2022**, *7* (11), 1042–1051.
- (10) Cameli, F.; Dimitrakellis, P.; Stefanidis, G. D.; Vlachos, D. G. Non-Oxidative Ethane Dehydrogenation in a Packed-Bed DBD Plasma Reactor. *Plasma Chem. Plasma Process.* **2023**, *43* (6), 2065–2078.
- (11) Wang, N.; Otor, H. O.; Rivera-Castro, G.; Hicks, J. C. Plasma Catalysis for Hydrogen Production: A Bright Future for Decarbonization. *ACS Catal.* **2024**, *14* (9), 6749–6798.
- (12) Cameli, F.; Dimitrakellis, P.; Vlachos, D. G. Direct Conversion of Ethane to Oxygenates, Ethylene, and Hydrogen in a Noncatalytic Biphasic Plasma Microreactor. *ACS Sustainable Chem. Eng.* **2023**, *11* (21), 8003–8008.
- (13) Ghosh, J.; Morato, N. M.; LeFever, W. A.; Cooks, R. G. Accelerated and Green Synthesis of N,S- and N,O-Heterocycles in Microdroplets. *J. Am. Chem. Soc.* **2026**, *148*, 2920.
- (14) Chen, H.; Yuan, X.; Zhang, J.; Chen, X.; Francisco, J. S.; Meng, Y.; Zhang, X. Simultaneous Reduction and Oxidation of NO₂ on Water Microdroplets Provides Previously Unknown Pathways to the Formation of HONO and HNO₃. *J. Am. Chem. Soc.* **2025**, *147* (42), 38500–38507.
- (15) Spoorthi, B. K.; Debnath, K.; Basuri, P.; Nagar, A.; Waghmare, U. V.; Pradeep, T. Spontaneous weathering of natural minerals in charged water microdroplets forms nanomaterials. *Science* **2024**, *384* (6699), 1012–1017.
- (16) Yu, W.; Ma, Y.; Yang, L.; Zhou, Y.; Liu, X.; Dai, Y. Electrostatic protein condensates as intracellular electrochemical reactors. *Nat. Mater.* **2026**, *1* DOI: 10.1038/s41563-025-02434-0.
- (17) Jia, M.-Y.; Zhou, Y.-W.; Yang, J.-L.; Liu, Q.; Cai, Z.-F. Catalyst-free Ullmann coupling in aqueous microdroplets. *Nat. Commun.* **2025**, *16* (1), 7453.
- (18) Wei, S.; Wan, Q.; Zhou, S.; Nie, W.; Chen, S. Spontaneous Generation of -CH₂CN from Acetonitrile at the Air-Water Interface. *J. Am. Chem. Soc.* **2024**, *146* (47), 32777–32784.
- (19) Grooms, A. J.; Huttner, R. T.; Stockwell, M.; Tadese, L.; Marcelo, I. M.; Kass, A.; Badu-Tawiah, A. K. Programmable C-N Bond Formation through Radical-Mediated Chemistry in Plasma-Microdroplet Fusion. *Angew. Chem., Int. Ed.* **2025**, *64* (4), No. e202413122.
- (20) Eldeeb, A. M.; Berbille, A.; Dick, J. E. No Microdroplets? No Problem. Soap Films Amplify the Interface and Produce Hydrogen Peroxide. *J. Am. Chem. Soc.* **2025**, *147* (37), 33325–33329.
- (21) Nandy, A.; Banerjee, S. Aqueous Microdroplets Induce the Metamorphosis of Indole into Quinazolinone Pharmacophores. *J. Am. Chem. Soc.* **2025**, *147* (45), 41242–41247.
- (22) Lee, K.; Cho, Y.; Kim, J. C.; Choi, C.; Kim, J.; Lee, J. K.; Li, S.; Kwak, S. K.; Choi, S. Q. Catalyst-free selective oxidation of C(sp³)-H bonds in toluene on water. *Nat. Commun.* **2024**, *15* (1), 6127.
- (23) Gan, T.; Yang, Z.; Li, S.; Qian, H.; Li, Z.; Liu, J.; Peng, P.; Bai, J.; Liu, H.; Wang, Z.; Wei, D. Unveiling Janus Chemical Processes in Contact-Electro-Chemistry through Oxygen Reduction Reactions. *J. Am. Chem. Soc.* **2025**, *147* (29), 25407–25416.
- (24) Shi, L.; LaCour, R. A.; Qian, N.; Heindel, J. P.; Lang, X.; Zhao, R.; Head-Gordon, T.; Min, W. Water structure and electric fields at the interface of oil droplets. *Nature* **2025**, *640* (8057), 87–93.
- (25) Lin, S.; Chen, X.; Wang, Z. L. Contact Electrification at the Liquid-Solid Interface. *Chem. Rev.* **2022**, *122* (5), 5209–5232.
- (26) Li, F.; Lv, J.; He, A.; Xu, J.; Zhao, L.; Wang, X.; Mao, L.; Li, S.; Wang, H.; Wang, Y.; Jiang, G. Unexpected Generation of Singlet Oxygen at the Air-Water Interface of Aqueous Microdroplets. *J. Am. Chem. Soc.* **2025**, *147* (34), 30574–30581.
- (27) Jin, S.; Chen, H.; Yuan, X.; Xing, D.; Wang, R.; Zhao, L.; Zhang, D.; Gong, C.; Zhu, C.; Gao, X.; Chen, Y.; Zhang, X. The Spontaneous Electron-Mediated Redox Processes on Sprayed Water Microdroplets. *JACS Au* **2023**, *3* (6), 1563–1571.
- (28) Meng, Y.; Xia, Y.; Xu, J.; Zare, R. N. Spraying of water microdroplets forms luminescence and causes chemical reactions in surrounding gas. *Sci. Adv.* **2025**, *11* (11), No. eadt8979.
- (29) Xia, Y.; Xu, J.; Li, J.; Chen, B.; Dai, Y.; Zare, R. N. Visualization of the Charging of Water Droplets Sprayed into Air. *J. Phys. Chem. A* **2024**, *128* (28), 5684–5690.
- (30) Kumar, A.; Avadhani, V. S.; Nandy, A.; Mondal, S.; Pathak, B.; Pavuluri, V. K. N.; Avulapati, M. M.; Banerjee, S. Water Microdroplets in Air: A Hitherto Unnoticed Natural Source of Nitrogen Oxides. *Anal. Chem.* **2024**, *96* (26), 10515–10523.
- (31) Meng, Y.; Gnanamani, E.; Zare, R. N. Water Droplet Microlightning Sparks Alkyne Ozonolysis. *J. Am. Chem. Soc.* **2025**, *147* (27), 23399–23404.
- (32) Xia, Y.; Meng, Y.; Shi, J.; Zare, R. N. Unveiling ignis fatuus: Microlightning between microbubbles. *Proc. Natl. Acad. Sci. U.S.A.* **2025**, *122* (41), No. e2521255122.
- (33) Ye, C.; Liu, D.; Gao, Y.; Liu, F.; Xu, H.; Jiang, T.; Wang, Z. L. Electrostatic breakdown at liquid-solid-gas triple-phase interfaces owing to contact electrification. *Matter* **2025**, *8* (4), 102007.
- (34) He, Y.; Meng, Y.; Zare, R. N. Positively Charged Water Microdroplets Ionize Surrounding Gas Molecules. *J. Am. Soc. Mass Spectrom.* **2025**, *36* (9), 1856–1859.

- (35) Peng, P.; Wang, Z. L.; Wei, D. Modulating multi-ion dynamics for high-performance iontronic systems. *Iontronics* **2026**, *2*, 5.
- (36) Ranasinghe, S.; Martin, C. D.; Dutton, J. L. Cyclopentadienyl cations. *Chem. Sci.* **2025**, *16* (5), 2083–2088.